

Experimental Study of Condensation Characteristics on a Vertical Plate Covered with Metal Foam

Ayser Muneer Flayh¹, Faik Hamad²

¹Department of Mechanical Engineering, College of Engineering, University of Baghdad, Baghdad, Iraq

²School of Computing, Engineering, Digital Technologies, Teesside University, Middlesbrough, Tees Valley, United Kingdom

Corresponding Author Email: aysar.m@coeng.uobaghdad.edu.iq

ABSTRACT

Metal foam (MF)-metal plate possesses the advantage of a big surface area; thus, it has great potential to improve the heat transfer on the surface of the condensation plate. In the current research, the heat transfer (HT) and pressure drop (ΔP) of water steam condensation on a vertical plate with copper foam (CF) were calculated with two different pore sizes (10 and 20 PPI) and the porosity of 90%. The steam mass flow rate is (0.005-0.009 kg/sec), and the range of cooling water rates is (0.1, 0.15, and 0.2 kg/sec). The correlations of HT and PD for a vertical flat plate (FP) with fixed CF are determined by the curve-fitting of the investigational values. Additionally, the results elucidated that the CF introduction improves the HT at a rate of 70% compared to the metal plate without copper foam, despite causing a bigger ΔP . A (10 PPI) sized CF reveals a higher performance. It is also observed that the higher pressure of inlet steam, the higher rate of the mass flow of steam, and the lower temperature of cold water will result in the increase of the overall heat transfer rate (HTR) as (49%) at 10 PPI and (41%) at 20 PPI.

Keywords:

Flat plate; Copper foam; Heat transfer; Pressure drop; Condensation steam

1. Introduction

Recently, many industries have inserted the application of heat energy transfer. Enhancements of HT methods include adding metal foam in Heat Exchanger (HE), decreasing of thermal boundary layer thickness, increase surface area, and increase the rate of HT. In addition, the composite systems of HT and the fluid flow that contains concurrently fluids and porous zones have taken substantial care in many industries owing to their significance in numerous uses, like micro-porous, HEs petroleum treating, or solid matrix. The Convection Heat Transfer (CHT) study into Porous Media (PM) inside a channel is a usual and significant problem. In numerous researches, the flow of fluid and the HT into channels incompletely filled with porous plates were scrutinized as investigational, numerical, and analytical. Y. P. Du et al. [1] studied numerically that a double HE filled with a MF. Eventually, the geometric factors of the HT and Metal Foam (MF) were investigated for studying their effects upon the dimensionless extra temperature at the mid position into axial direction, as well as the complete HT performance of HE. The results demonstrated that the ratio of length to inner diameter was elongated to around (180), and a (0.6 - 0.7) range for the dimensionless internal tube dia. ($R1/R3$) was indorsed for the design of MF filled with HEs. Mohamed A. et al. [2] studied the force-convection flow of a tube filled completely or partially with Metallic Porous Media (MPM) for three cases. The study examined the impact of dimensionless outer radius of the MPM ($0 \leq R_{pe} \leq 1$) as well as Darcy no. ($2 \times 10^{-4} \leq D_a \leq 2 \times 10^{-1}$) upon the profiles of velocity, Nusselt no. (Nu), average Nusselt no. (Nu_{avg}), and (ΔP) while maintaining constant values for Prandtl no. (Pr), Reynolds no. (Re), and Porosity (ϵ). An annular flow pattern based on the modified microstructure model was used to investigate analytically by Du et al. [3] the air flow in a tube filled by foam.

A virtuous covenant was achieved between the analytical and the experimental outcomes of Zhao et al. [4]. K. Senthilkumar and P. Palanisamy [5] investigated the HTC of a double-pipe HE, arrangement as introducing a different PM upon the outside surface of the DPHE internal tube wall employing Wilson's plot analysis. The exhaust gas and water from a twin cylinder diesel engine were used. Also, the circulation of flow evolves a turbulent motion which causes a rise HTC. In addition, the investigational examinations were performed upon the evolved developed DPHE with (4) various PM chosen as aluminum, copper, mild steel and cast iron. Furthermore, the HTC was scrutinized employing the correlations of Wilson's plot technique as well as the Nu. Moreover, the outcomes with Wilson's plot technique and the investigational outcomes were obtained with virtuous covenants. Hui Wang et al. [6] showed the experimental results, using a Double-Pipe Heat Exchanger (DPHE), and the tube is filled with a stainless steel foam (10, 30, and 70 PPI), as for the porosity is 39%. The air flow of velocity is 7.0 to 26.0 m/s inside the tube. The results demonstrated that the Nu obtained under convective boundary condition is much lower than that obtained under constant heat flux boundary condition. Shahram et al. [7] studied experimentally a forced CHT of a single-phase flow air into a channel possessing a circular cross-section with various arrangements of PM that influence on the PD and the HTR. The results showed that the bigger HTRs value can be attained via raising the PM dia. as well as raising the rate of air flow. From these results, it can be shown that the improved HT was carried out when the diameter of PM was close to the diameter of the channel. Hossein A. et al. [8] investigated the HTR and air flow in a double-pipe, counter-flow HE using partially MF inserts, targeting to optimize the MF distribution for maximum HTR and minimum ΔP . It was found that the HE's efficacy, HTR, overall HTC, and effectiveness can be enhanced by up to 69, 124, and 9%, respectively. S. Ahmadi et al. [9] examined the effect of surface wettability of metal foams upon the HT and the PD of R 134 refrigerant condensing flow in tubes. The obtained results portrayed that the hydrophobic MFs increased the HTC till (39%) and decreased the frictional ΔP till (15%). Also, the hydrophilic MFs rose the HTC and ΔP till (32%) and (38%), correspondingly. Luyi Li [10] studied the effect of PPI value (10, 15, and 20), steam-air mixture flow rate, and non-condensation gas on HTC and resistance of flow in a pipe filled with metal foam. The results show that the tube filled with 10 PPI copper foam has the highest HTC compared to the smooth pipe.

Metal foams have been found to exhibit promising HT for use in HEs owing to their intricate geometry as well as elevated surface area-to-volume ratio, and so on. Such influences improve the HT performance, but simultaneously, presumably owing to such elevated intricate structure, the retention of steam condensation may be difficult. The up-to-date literature survey revealed that there are only a few experimental studies to steam condensation on a vertical plate covered with metal foam (MF). In the present study, the heat transfer rate (HT), pressure drop (ΔP), and overall heat transfer coefficient of water steam condensation on a vertical plate with copper foam (CF) were calculated with two different pore sizes (10 and 20 PPI) and the porosity of 90%.

2. Experimental Apparatus and Procedure

The practical study was conducted in a test rig depicted in the figure 1. The test rig was built into the laboratory of fluid. It consists of the following major assemblies:

- A boiler that generates a vapour with the given flow rate.
- A cold tank that provides the cooling capacity for steam condensation.
- Installation of aluminium plate covered without, and with CF with various structures.

The investigational system's schematic diagram is shown in figure 1 and, the test rig was a rectangular shell, produced of transparent Perspex having a width, height, and length (500 mm, 250 mm, and 405mm), correspondingly. The test condenser within the shell comprises a smooth-plate of aluminum with width 200 mm, length 300 mm, and thickness 3 mm covered with two types of pore's density (10 PPI and 20 PPI) and porosity 90% which is the same as a plate dimension but with a different thickness (10 mm) is shown in figure 2. In the plate of condenser, the condensation water drained off the surface of plate was accumulated in a condensate tray and drained through the drain tube. The test rig was equipped with purging port for removing the non-condensable, i.e. air, and at the beginning of the experimentation, it should vent every non-condensable. The left out non-condensable vapor was removed from the condenser surface employing a steam separator. The pressure into steam separator was less than that into rectangular shell.

Consequently, the non-condensable along the steam were gushed down to the steam separator, from where they're vented off through a valve. The estimation exhibited that the steam separator was about 20% of the steam being condensed into the chief condenser.

For cooling water circulation into the test rig, which will come from a cooling water tank, was offered with an overflow pipe for maintaining a fixed connecting the tank of cooling water to condenser plate. Such a pump circulated the water into the condenser plate of the test section (TS). The flow rate of cooling water into the test section was measured via Rotameter. The hydro-dynamic stabilization [10, 11] of the flow of cooling water was attained via offering thermal isolated pipes having a length of $(50 D_i)$ upon the upstream side as well as $(20 D_i)$ upon the downstream side of TS. Also, the hot water that flows out from the surface of condenser was accumulated into a tank of hot water and eventually drained off by valve. As well, the electrically heated boiler was utilized for generating the steam which being provided to the TS through the copper hoses. The steam left the boiler and was flushed during a drain pipe connecting valve that was opened. The pipeline's connecting valve's free end possessed a trap of steam. Also, the steam was permitted to go into the test rig beyond regulating the pressure to a pre-determined value into the pressure regulator. Later, a steam meter (vortex flow meter) was utilized for measuring the rate of the mass flow of inlet steam. Additionally, for safety purposes, a vent valve was positioned upon the tank's top to avoid every elevated pressure of the steam that was trapped in the boiler, regulate the rate of steam flow to the test rig, and remove every extra steam via employing a bypass valve.

Two sheathed K-type thermocouples having a precision of $(\pm 0.15^\circ\text{C})$ for measuring the coolant's temperature difference between inlet and outlet were fixed at the two TS sides (plate with and without MF). The wires of the K-type thermocouple were fitted at four lines (upper, mid 1, mid 2, and lower) on the flat plate for measuring the wall's temperature. Also, a drain valve is fixed at the TS exit, which merely permits the condensate (in place of extra steam) for draining from the condensation chamber's bottom to an electronic scale, as well as by weighing the mass of condensate in a given time with this scale, the rate of the condensate water's mass flow can be measured.

2.1 Metal Foam

Metallic porous media (MPM) of open-cell high porosity was used in the experiments. An inner tube shape HE was provided with metallic porous tube at different pore densities of (10 PPI and 20 PPI) as well as having the same porosity of 90%, as shown in figure, 1(C).

2.2 Experimental Procedures

The experimentations were recurrent with changing the operating factors to investigate their influence upon the ΔP , coefficient of HTR, and temperature distribution. These parameters are:

- Feed water flow rate range (0.1, 0.15 and 0.2 kg/sec).
- Feed water steam rate range (0.005, 0.006, 0.007, 0.008, and 0.009 kg/sec).
- Inlet temperature of water steam supply (100°C).
- MF range (10, 20 PPI, and 0 PPI (plain pipe)).

The experiments were initiated via working the pump and regulating the needed rate of the water flow which was attained via a valve of flow, and the electrical power was then switched on, as well as the input voltage of heaters was regulated by a transformer (Variac). This device was remained as a minimum for one hour for reaching the steady-state circumstance [11], and the water steam rate in the TS achieved a steady state very rapidly allowing measuring of the following data to commence immediately. Every half an hour, the thermocouples readings were recorded via the data logger regime, till the reading got nearly fixed (the temperature didn't change via $(> 0.5^\circ\text{C})$ into thirty min), the last reading was registered at the steady-state circumstance. Throughout every run of test, the following readings were registered:

- Heater power watt;
- Water steam rate kg/sec;
- Cooling water rate kg/sec;
- The inlet and outlet temperature of water steam and cooling water, $^\circ\text{C}$;
- Metal foam temperature (upper, mid 1, mid 2, and lower), $^\circ\text{C}$; and
- PD across the MF by pressure gauge in Pa.

The same procedure was repeated for various cooling water flow rates, hot water, and different MFs.

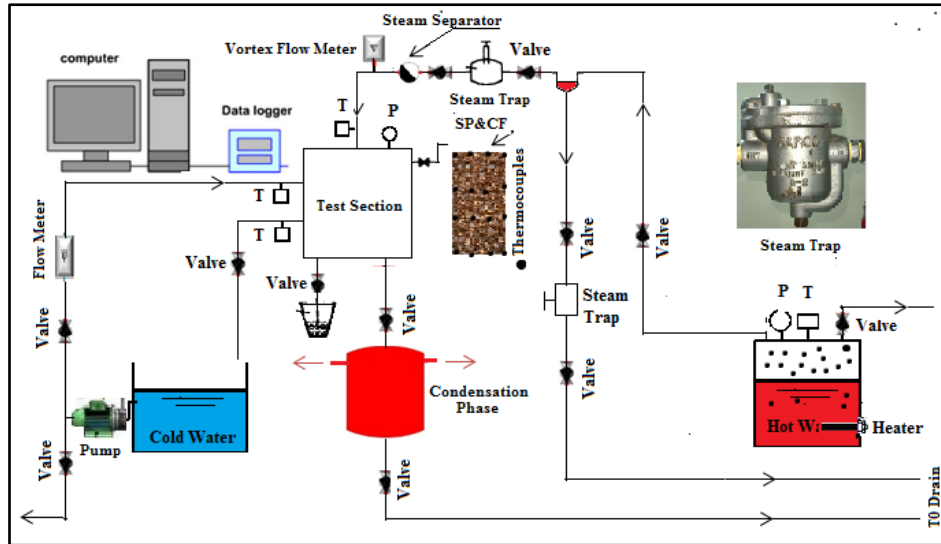


Figure1. Schematic Diagram of the Experimental



Figure2. Test Plate with CF (10 and 20 PPI) and without CF (Smooth Plate)

3. Data Reduction Equations

The following assumptions are taken under consideration during modeling the case study:

- The HT between the cold water and steam water is time independent and incompressible flow.
- The HT due to convection of natural and radiation are neglected.
- The thermo physical properties are constant and the temperature of air flow is negligible.

The experimental HTR (Q_c) and the average heat flux (q) in the HE can be computed using the subsequent equations [12]:

$$q = \frac{Q_c}{a} \quad (1)$$

$$Q_c = \dot{m}_c C_{pc} (T_{in,c} - T_{out,c}) \quad (2)$$

$$a = l \times W \quad (3)$$

$$T_c = \frac{T_{in,c} + T_{out,c}}{2} \quad (4)$$

Where, a is the plate condensation of the area, T_c is the water temperature cooling average, $T_{in,c}$ and $T_{out,c}$ are inlet and outlet cold water temperature, \dot{m}_c is mass flow rate of cold water, and C_{pc} is the thermal capacity of cold water.

This equation calculates the HTC (h) average:

$$h = \frac{q}{T_s - T_w} \quad (5)$$

$$T_s = \frac{T_{in,s} + T_{out,s}}{2} \quad (6)$$

$$T_w = \frac{\sum_n T_{wn}}{n} \quad (7)$$

$$T_{wn} = \frac{T_{upper,n} + T_{lower,n} + T_{left,n} + T_{right,n}}{4} \quad (8)$$

Where, T_s is the steam temperature average, T_w is the wall surface temperature average. Latent heat of steam condensation rate ($q_{cond.}$) could be calculated as [13]:-

$$q_{cond.} = \dot{m}_s h_{fg} \quad (9)$$

The modified latent heat (h_{fg}) is defined as:

The overall HT (U) of a metal plate covered by a CF can be computed as following:

$$U = \frac{q_{cond.}}{a (T_s - T_{w,avg.})} \quad (10)$$

4. Initial Measurements

CF is a kind of PM and it's necessary to measure the chief properties experimentally for specifying the precise circumstances, which are porosity, permeability, and effective thermal conductivity that are preceded by the present experimental work.

4.1 MF Porosity

Porosity (ϵ) is the significant MFs property, that of which it relies upon the total sample volume that contains CF and pores volume. A sample from CF having a specific volume was taken and introduced into the pipe. The pipe mass into a dehydrated state was measured. It was then filled with water, and it was shaken gently to safeguard that the water engulfed the voids between the matrices of pores. Also, the saturated configuration mass was measured. Additionally, the discrepancy in pipe with the mass of MF after and before the saturation was the mass that filled the CF pores, as well as if separated via the pure copper's theoretical density ($\rho = 8933\text{kg/m}^3$) [14]. Then, ϵ can be shown using this equation:

$$\epsilon = \frac{V_{void}}{V_{solid}} = 1 - \frac{V_{solid}}{V_{total}} \quad (11)$$

4.2 Permeability of the MF

The PM of fluid flow was described by [3]. The subsequent Forchheimer prolonged Da's law was used for a laminar and steady state, unidirectional (ΔP) in a uniform, homogeneous, and isotropic PM, as well as Newtonian and Incompressible liquid flow [4].

$$\frac{\Delta P}{l} = \frac{\mu}{K} U + \frac{\rho c}{\sqrt{K}} U^2 \quad (12)$$

The terms $\frac{\mu}{K}$ and $\frac{\rho c}{\sqrt{K}}$ represents Darcy number and Forchheimer number, respectively.

Assuming that is totally developed, as well as the viscous flow influences are small, and of that, the equation of momentum could be solved as:

$$\frac{\Delta P}{l} = AU + BU^2 \tag{13}$$

When comparing Equation (12) with equation (13), permeability and inertial coefficient respectively can be written for each MF block as:

$$K = \frac{\mu}{A} \tag{14}$$

$$C = \frac{B\sqrt{K}}{\rho} \tag{15}$$

Permeability (K) as well as inertial coefficient (C) of every MF blocks is practically obtained via measuring the pressure drop (ΔP) crossways the test rig at various rates of the flow of air. For finding K and C for every MF block, the constants A and B into Equation (13) have to be computed via creating a curve fitting (2nd-Order Polynomial), as evinced into Figure (3). Table 1 lists the values of A and B for every curve. The (K) and (C) values for each MF block are given in Table 2.

5. Solid-Fluid Combined Media Thermal Properties

5.1 Effective Thermal Conductivity

The effective conductivity (K_{eff}) from the MF case has to be computed for determining the effective HTC. Such (K_{eff}) is obtained employing Equation (16) [2]:

$$K_{eff} = (1 - \epsilon)K_s + \epsilon K_f \tag{16}$$

Where, K_s and K_f are the conductivity of the solid and fluid, respectively.

5.2 Mean Heat Capacity

The saturated PM of the fluid and the solid heat capacity amalgamation can be evaluated as the weighted-arithmetic mean of the fluid and the solid heat capacity, in accordance with:

$$(\rho C_p)_{mean} = \epsilon(\rho C_p)_{fluid} + (1 - \epsilon)(\rho C_p)_{solid} \tag{17}$$

$(\rho C_p)_{mean}$ is the media mean heat capacity. While $(\rho C_p)_{fluid}$ represents the heat capacity of fluid saturated, and $(\rho C_p)_{solid}$ accounts the heat capacity of solid matrix.

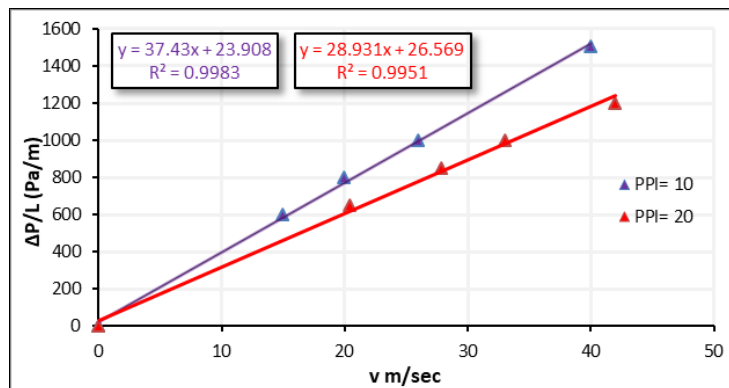


Figure 3. Variation of Pressure Drop across The Metal Foam with The Velocity at The Inlet.

Table 1. Rates of The Constants (A and B)

Pores Per Inch (PPI)	A	B
10	23.908	37.43
20	26.569	28.931

Table 2. Measured Permeability, ICMF, and Da

Pores Per Inch (PPI)	Permeability (m ²)	Inertial Coefficient (C)	Darcy No. (Da)
10	7.73×10^{-7}	0.0281	9.82×10^{-4}
20	6.39×10^{-7}	0.0197	8.15×10^{-4}

6. Uncertainties

The main uncertainty comes from the measurements of temperature, pressure, and the values of mass flow. Thermocouples (K-Type) were utilized during the test setup, and the measured temperature uncertainty is ($\pm 1.4^\circ\text{C}$). Also, the measured pressure uncertainty is up to ($\pm 5\%$). Additionally, the uncertainty of the difference in pressure is ($\pm 5\%$). The uncertainties in such experimentation are summarized in Table 3. Furthermore, the uncertainty in computing the overall HTC is computed depending upon the traditional approaches of error spread.

Table 3. Uncertainties of Experimental Parameters

Parameters	Range	Uncertainties
Water steam temperature $^\circ\text{C}$	10-130	± 0.15
Plate surface temperatures $^\circ\text{C}$	10-130	± 0.15
Cooling water mass flow rate kg/sec	0-1	$\pm 5\%$
Steam flow rate kg/sec	0-1	$\pm 2\%$
Steam pressure MPa	0-0.1	$\pm 5\%$
Overall Heat transfer coefficient $\text{W/m}^2 \text{K}$	1000-4500	$\pm 5\%$

7. Results and discussion

The effect of the following parameters' ranges on the HTR, overall HTC, and ΔP was investigated in the experimental parts:

1. Metallic porous media porosity, PPI ranges (10 and 20 PPI), and porosity 0.9.
2. Water steam flow rate range (0.005, 0.006, 0.007, 0.008, and 0.009 kg/sec).
3. Cold water flow rate range (0.10, 0.15, and 0.20 kg/sec).

7.1 Temperature Distributions

The flow pattern of the water steam on the flat plate (FP) covered with a metal foam has a great influence on the HT. In accordance with the fluctuation and distribution of the temperature of the wall, the flow pattern is predicted. The investigational outcomes manifested that the influence of the value of copper foam PPI possesses a slight influence upon the pattern of flow. By taking flow condensation on the flat plate covered with different metal foam PPI, and the steam flow pattern on a flat plate without CF, the key observations are summarized as follows:

When the rate of water steam is (0.005 kg/sec), the flow pattern is observed, with constant cold water mass flow rate of (0.1 kg/sec), and the average cooling water temperature is 30°C . The temperature was measured at four

linear places which are lower (T_{lower}), mid1 (T_{mid1}), mid2 (T_{mid2}), and upper (T_{upper}) at the cross-sectional area (20 thermocouples sensor taps were distributed uniformly four by five at 20 locations positioned along plate axial direction). Figures 5, and 6 illustrate the measured temperatures along the plate without and with using of the CF. The T_{upper} and T_{mid1}/T_{mid2} were recorded higher than the T_{lower} . T_{upper} and T_{mid1}/T_{mid2} along the plate fluctuating, the temperature at lower surface (T_{lower}) reduces lengthways the flat plate length. Temperature differences among the four locations, on the entrance of the test section plate for all studied cases, were within a range of 14°C. The steam has a lower density than condensed water, thus it will accumulate in the upper zone of the inner plate. While, the T_{mid1} and T_{mid2} have a similar temperature at the inlet, because the steam part was more than the condensed water at the plate entrance, though the temperature gradually drops along the test section. The behavior of T_{mid1} and T_{mid2} should be identical because they have symmetrical location. The slight deviation between of their measurements might be attributed to an error in the sensors. The T_{lower} at the entrance has a similar value and close to the steam saturation temperature; however, the temperature decreases gradually. This slight drop in temperature is due to the gravity that pulls down the condense water, and the film thickness keeps constant in the entire upper half of plate, while it gets thicker at the bottom, this behaviour was also stated by other published work [15]. In general, the configuration for all curves show that the temperature decreases towards the end of heat exchanger due to heat transfer from hot steam to cooling water. Also, the surface temperature reduces in cases that use metal foam as a porous media, when it compared to the cases of without using the metal foam is shown in figure 4. The drop in temperatures on the surface, due to use the metal foam increases surface area and mixing of the fluid. Further, it can be also seen that, the temperature of the minimum steam flow rate is the same as the less surface temperature along the inner plate, where the increasing in the mass flow rate increase in surface temperature. Furthermore, because the increasing in inlet velocity, it leads to change a vortex form of the working fluid on the surface of the plate, which has substantial effect on the performance of heat transfer, or give more turbulence in the steam flow, hence lead to high HTC [16].

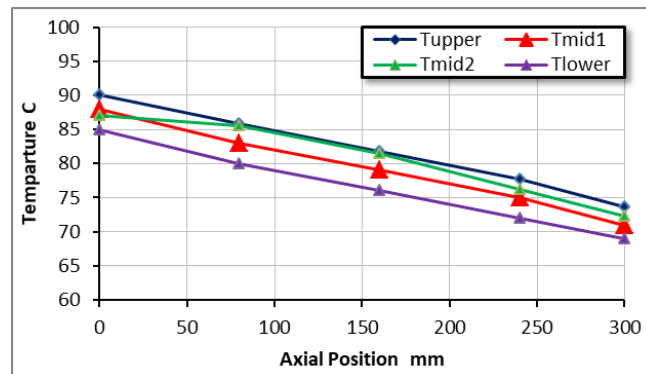


Figure 4. Distribution of the Wall Temperature of Steam (0.005 kg/sec) and Cold Water (0.1 kg/sec) without CF

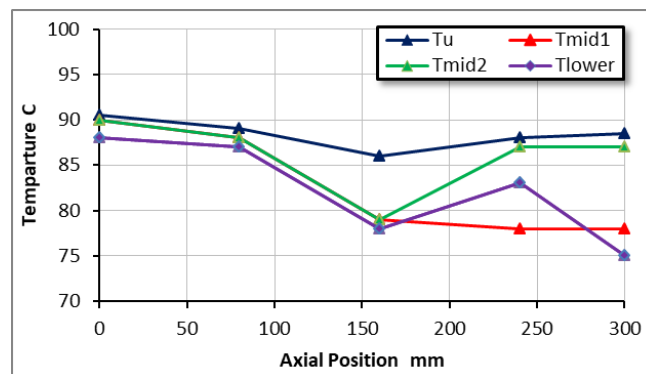


Figure 5. Distribution of the Wall Temperature of Flow on the Plate Covered with CF (10 PPI) at Steam (0.005 kg/sec) and Cold Water (0.1 kg/sec).

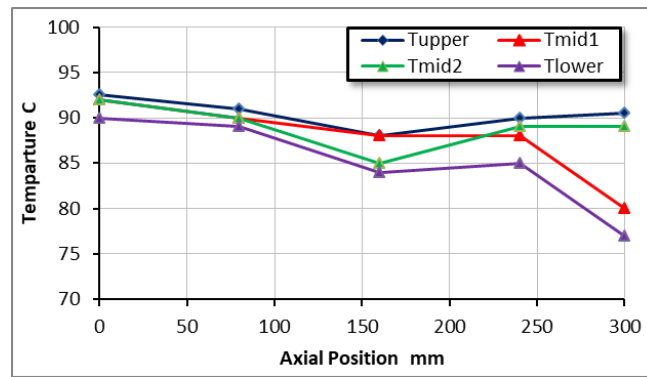


Figure 6. Distribution of The Wall Temperature of Flow on The Plate Covered with CF (20 PPI) at Steam (0.005 kg/sec) and Cold Water (0.1 kg/sec).

7.2 Temperature difference:

Figures 7, 8, and 9 elucidate the differences between steam temperature at the inner and outer against the flow rate of water steam. The large amount of cooling flow rate and a lesser amount of steam flow rate lead to lowering the temperature difference of the tube wall alongside with the HT rising, hence increasing the condensed liquid amount. The MF enhances the condensation process in average term for the range of used steam mass flow rates about 12.2%, 12.3%, and 15.3% for 0.1, 0.15 and 0.2 kg/sec of the cold-water flow rate, respectively. Thus, it could be forecast that the CF could have a good possibility in the condensation flow. The maximum value of the enhancement of different temperatures (T_{diff}) in the cases 20 PPI and 10 PPI from a smooth plate was 15% and 18.5%, respectively, at the cold water flow rate of 0.1 kg/sec. At a cold water flow rate of 0.15 and 0.2 kg/sec, the maximum improvement rate was 16% and 21%, or 17% and 24%, at (20 PPI) and (10 PPI), respectively.

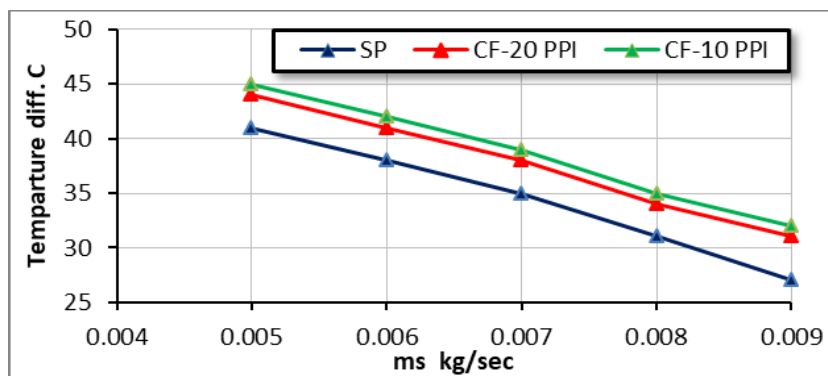


Figure 7. Variations of The Different Temperatures ($T_s - T_{w,avg}$) of the HE with The Rate of The Mass Flow of without CF and with CF at Cold Water=0.10 kg/sec.

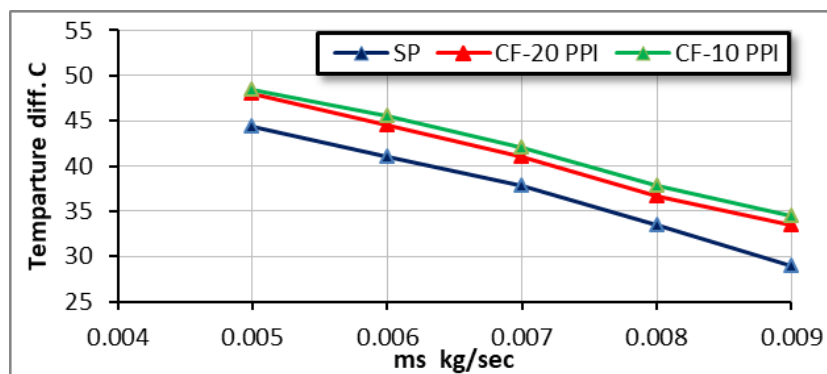


Figure 8. Variations of The Different Temperatures ($T_s - T_{w,avg}$) of the HE with the Rate of The Mass Flow of without CF and with CF at Constant $m_c=0.15$ kg/sec.

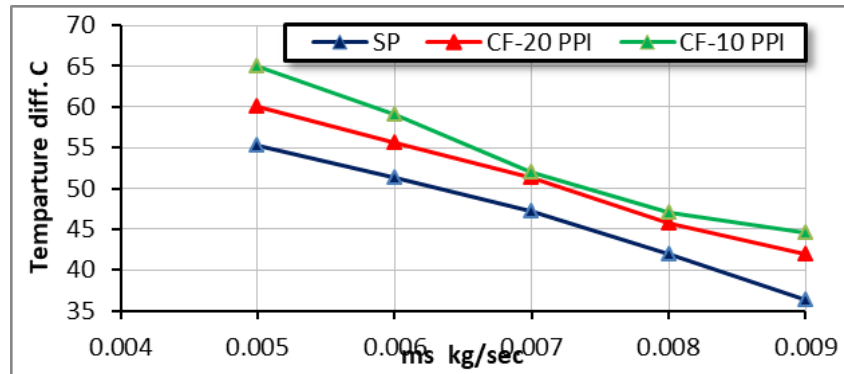


Figure 9. Variations of the Different Temperatures ($T_s - T_{w,avg}$) of HE with the Rate of the Mass Flow of without CF and with CF at Constant $m_c=0.2$ kg/sec.

7.3 Heat Transfer Rate (HTR)

The influence of the pore's density of MF upon the average heat transfer rate HTR is displayed in the figure 10. The cooling temperature of water is (30°C), and the temperature rate of the water steam is (90°C). Also, the HTR of water steam flow into MF-FP is greater than that into a plate, owing to the elevated HT area. If the rate of mass flow is more than (0.005 kg/sec), the HTR of water steam flow into (20 PPI) MF-FP is almost once and double into the (10 PPI) MF plate with the similar geometry. Additionally, from this figure, it can be noted that the HTR rises with the decrease of pore's density of CF (PPI). Though, the pore size of (10 PPI) surface area is less than the pore size of (20 PPI). If the temperature of cold water is fixed, the T_w varies gradually. In addition, the ΔT rising rate, the heat transfer rate (HTR) increases. Thus, the average reduces by raising the pressure of inlet steam, as observed by Equation (2) and as presented into the figure 10. The maximum heat transfer rate is up to 43kW at 10 PPI.

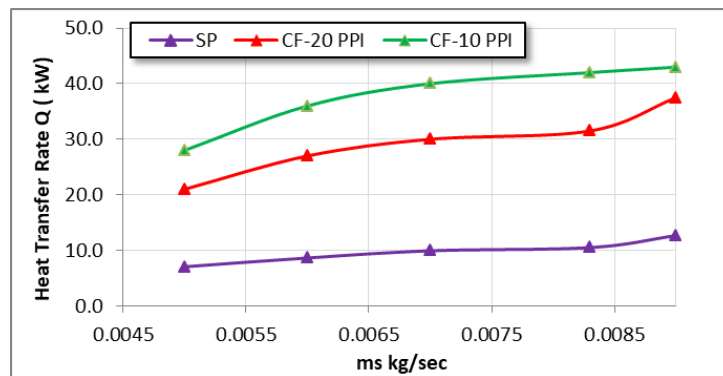


Figure 10. Influence of The Mass Flow Rate upon HTR on Plate Covered With CF at Selected Pore Densities

7.4 The overall heat transfer coefficient (HTC)

Figures 11 to 13 illustrate the effect of PPI variation and cooling water flow rate variation upon the overall HTC at the rate of the mass flow of the steam water and the cold water. These figures reveal that the HTR is inversely proportional to different pore densities (10 PPI and 20 PPI) as it increases gradually versus the mass flow rate of the steam water and the cold water increase, while it increases versus the different pore densities (10 and 20 PPI). For the cold water flow rates of 0.1, 0.15, and 0.2 kg/sec, the CF having a (20 PPI) pore's density has a relatively lower overall HTC than that with 10 PPI. The overall HTCs of 10 PPI and 20 PPI are identical, which are (47%-44%), (49%-41%), and (47%-40%), respectively, higher than the smooth plate without considering the uncertainty. Such trends may be related to the combined effects of the thickness of condensation films, the area of specific HF, and capillarity. A relatively larger difference in the HTCs is observed at lower rates of HT.

7.5 Pressure Drop (ΔP)

In figure 14, a pressure difference transducer was used to measure the ΔP . As anticipated, pressures drop rises when inserting CF hugely. The (10 PPI) CF pore's density rises the single-phase ΔP by till (1.7) times in comparison with the smooth-plate (without CF). The increase is by up to (4) times for the (20 PPI) MF pore's density. Raising the CF pore's density from (10 PPI) to (20 PPI) raises the ΔP till (17%).

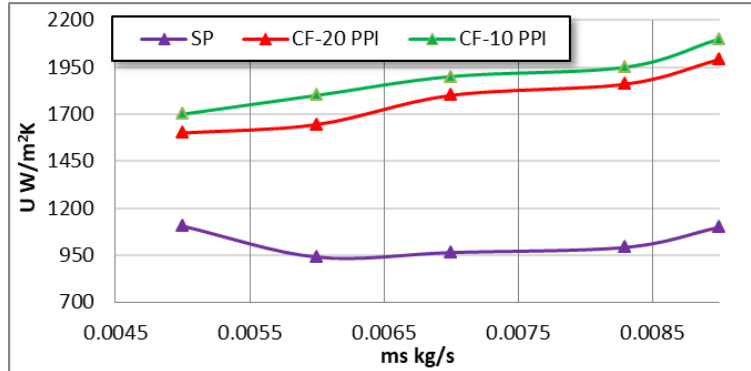


Figure 11. Variations of the Overall HTC of HE With the Mass Flow Rate of Steam Water at $m_c=0.10$ kg/sec.

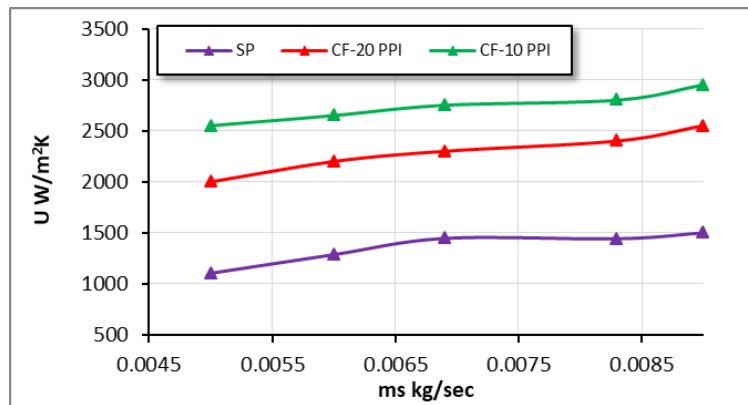


Figure 12. Variations of The Overall HTC of HE with The rate of The mass flow of steam water at $m_c=0.15$ kg/sec.

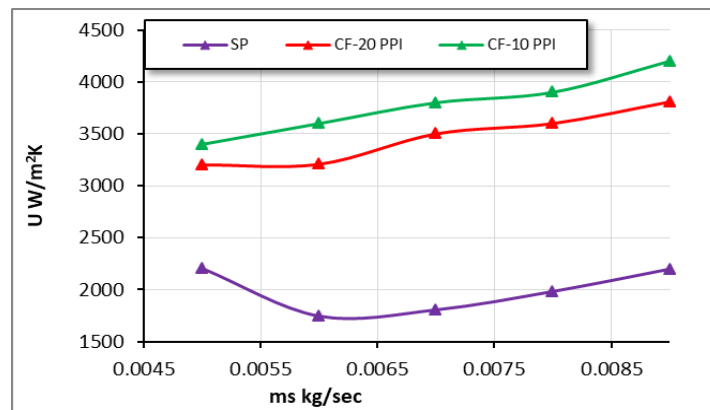


Figure 13. Variations of The Overall HTC of HE with The Rate of The Mass Flow of Water Steam at $m_c=0.2$ kg/sec.

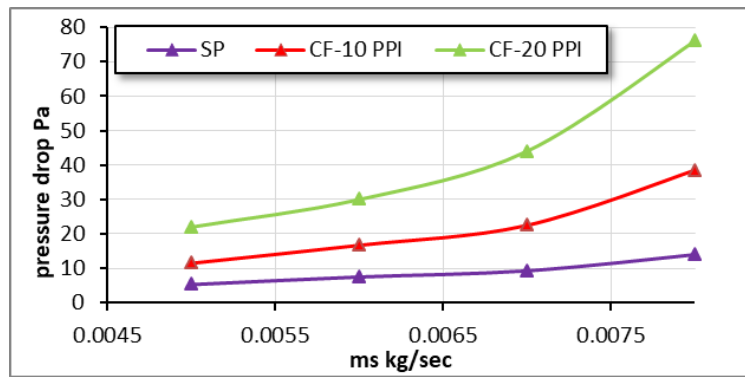


Figure 14, Pressure-Drop Curves for the CF Plotted Upon the Scale (ΔP) Against (m_s) .

7.6 Steam condensation

The volume flow rate of condensed liquid and steam was measured at different conditions. Figure 15 demonstrates a comparison between a condensed water flow rate, using 0.1, 0.15, and 0.2 kg/sec of the cold water, with or without enhancement by the CF, using 0.005, 0.006, 0.007, and 0.008 kg/sec of the water steam. While figure 16 manifests a comparison between the rates of the condensed water flow, with and without enhancement, using the cold water flow rate of 0.1, 0.15, and 0.2 kg/sec at 20 PPI under steam gauge pressure of 1 bar. Also, it can be seen in both figures that the condensed water volume increases with the increase of the rate of steam mass flow. The comparison between the results shown in these figures clearly portrays that the volumes of the condensed water increase with an increase in the rate of cooling water flow.. Furthermore, these figures present the CF effect on the condensation process enhancement.

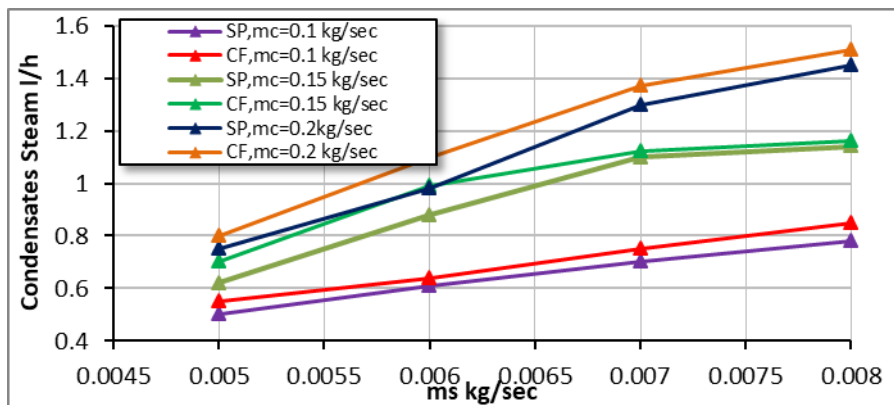


Figure 15. Condensation Water Flow Rate Against Steam Water Mass Flow Rate at 20 PPI.

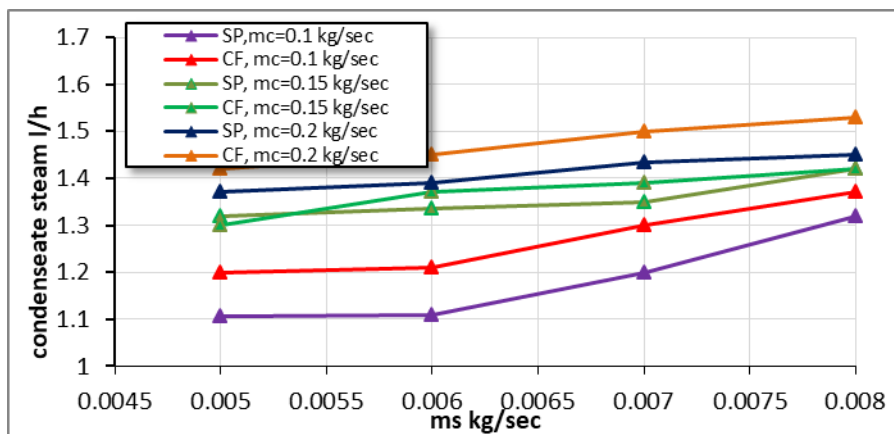


Figure 16. Condensation Water Flow Rate Against Steam Water Mass Flow Rate at 10 PPI.

8. Conclusions

The condensation HT of an aluminum plate with a CF having a pore's density of 10 PPI and 20 PPI was fixed on it, and the results were compared with the condensate plate without CF. The following conclusions draw from the experiment results are summarized as follows:

1. The HTRs of the condensation of an aluminium plate with a CF rise initially and reduce then with the PPI rise, and the (10 PPI) CF wrapped plate elucidated the optimum condensation improvement. The HTRs of condensation for (10 PPI) and (20 PPI) CF fixed FP are (70%) and (65%) larger than that of plate without CF, respectively.
2. The maximum value in the PD for 20 PPI in comparison with a smooth-plate (without CF) is found to be (76 Pa) at the cold water $m_c=0.2$ kg/sec and the steam water $m_c=0.09$ kg/sec.
3. The overall HTC can be improved as high as (49%) at 10 PPI, and (41%) at 20 PPI, at the cold water $m_c=0.15$ kg/sec.
4. The maximum value for condensate steam is (1.6 l/h) at 10 PPI and at the cold water $m_c=0.2$ kg/sec.

Declaration of Competing Interest

The author Ayser and author Faik declare that there are no conflicts of interest regarding the publication of this manuscript.

Funding Information

This research was not funded by any financial organization.

Author Contributions

Authors have suggested the search problem. The author, Faik, collected recent research related to the research problem and also recommendations to work on the proposal. In addition, the author Ayser designed the test section work and discussed it with the author Faik. The author, Ayser, discussed all the research output. Finally, the authors, Ayser and Faik, discussed the data results and the final version of this paper.

Acknowledgments

The authors express their gratitude to Baghdad University/ College of Engineering/Mechanical Engineering department in Baghdad-Iraq for supporting this study.

Nomenclature	Meaning
A	Constant coefficient
a	Surface Area, m^2
B	Constant Coefficient
C	Inertial coefficient
c_p	Thermal Capacity, kJ/kg K
h	Heat transfer coefficient, $W/m^2 K$
h_{fg}	Latent heat, J/kg
K	Permeability, m^2
l	Length of plate or metal foam, mm
\dot{m}	Mass flow rate, kg/sec
P	Pressure, Pa
Q	Heat transfer rate, W
q	Heat transfer flux, W/m^2
T	Temperature, K
V	Volume, m^3
U	Overall heat transfer coefficient, $W/m^2 K$
W	Width, mm

Greek symbols	Meaning
ϵ	Porosity
ρ	Density, kg/m ³
μ	Dynamic viscosity, Pa.s
Subscripts	Meaning
avrg.	Average
c	Cold water
cond.	Steam condensation
diff.	Different
f	Fluid
S	Solid
s	Water steam
w	Wall
Abbreviations	Meaning
HT	Heat Transfer
CF	Copper Foam
PD	Pressure Drop
FP	Flat Plate
HE	Heat Exchanger
HTC	Heat Transfer Coefficient
CHT	Convection Heat Transfer
PM	Porous Media
MF	Metal Foam
Da	Darcy Number
Nu	Nusselt Number
Nu _{aveg}	Average Nusselt Number
Pr	Prandtl Number
Re	Reynolds Number
HF	Heat Flux
DPHE	Double-Pipe Heat Exchanger
MPM	Metallic Porous Media

Reference:

- [1] Y. P. Du, Z. G. Qu, C. Y. Zhao, and W. Q. Tao, "Numerical study of conjugated heat transfer in metal foam filled double-pipe," *Int. J. Heat Mass Transf.*, vol. 53, no. 21–22, pp. 4899–4907, 2010.
- [2] M. A. Teamah, W. M. El-Maghlany, and M. M. Khairat Dawood, "Numerical simulation of laminar forced convection in horizontal pipe partially or completely filled with porous material," *Int. J. Therm. Sci.*, vol. 50, no. 8, pp. 1512–1522, 2011.
- [3] Y. P. Du, C. Y. Zhao, Y. Tian, and Z. G. Qu, "Analytical considerations of flow boiling heat transfer in metal-foam filled tubes," *Heat Mass Transf. und Stoffuebertragung*, vol. 48, no. 1, pp. 165–173, 2012.
- [4] C. Y. Zhao, T. Kim, T. J. Lu, and H. P. Hodson, "Thermal transport in high porosity cellular metal foams," *J. Thermophys. Heat Transf.*, vol. 18, no. 3, pp. 309–317, 2004.
- [5] K. Senthilkumar and P. Palanisamy, "A study of concentric tube heat exchanger with different porous particles using Wilson plot analysis," *Int. J. ChemTech Res.*, vol. 8, no. 10, pp. 138–147, 2015.
- [6] H. Wang and L. Guo, "Experimental investigation on pressure drop and heat transfer in metal foam filled tubes under convective boundary condition," *Chem. Eng. Sci.*, vol. 155, pp. 438–448, 2016.
- [7] S. Baragh, H. Shokouhmand, S. S. M. Ajarostaghi, and M. Nikian, "An experimental investigation on forced convection heat transfer of single-phase flow in a channel with different arrangements of porous media," *Int. J. Therm. Sci.*, vol. 134, no. September 2017, pp. 370–379, 2018.
- [8] H. Arasteh, M. R. Salimpour, and M. R. Tavakoli, "Optimal distribution of metal foam inserts in a double-pipe heat exchanger," *Int. J. Numer. Methods Heat Fluid Flow*, vol. 29, no. 4, pp. 1322–3142,

- 2019.
- [9] S. Ahmadi, M. A. Akhavan-Behabadi, B. Sajadi, and M. M. Ahmadpour, "Effect of hydrophilic and hydrophobic metal foams on condensation characteristics of refrigerant flow inside annular tubes: Experimental study," *Therm. Sci. Eng. Prog.*, vol. 40, no. 101785, 2023.
- [10] L. Li, "Experimental study on enhancement condensation heat transfer in tube by foam metal in presence of non-condensable gas," *J. Phys. Conf. Ser.*, vol. 2671, no. 1, 2024.
- [11] M. A. Al-Dhaher, M. H. Al-Mosawi, and A. T. Al-Sammarai, "An Experimental Study on Forced Convection Heat Transfer From An Embedded Horizontal Cylinders Array in A Porous Medium in Cross Flow," *Tikrit J. Eng. Sci.*, vol. 14, no. 2, pp. 1–31, 2007.
- [12] B. Bidar, F. Shahraki, and D. M. Kalhori, "3D Numerical Modelling of Convective Heat Transfer through Two-sided Vertical Channel Symmetrically Filled with Metal Foams," vol. 60, no. 4, pp. 193–202, 2016.
- [13] A. Muneer, "Film Condensation on a Vertical Tube at Different Pressures," *J. Eng. Appl. Sci.*, vol. 24, no. 13, pp. 241–253, 2017.
- [14] S. P. Venkateshan, "Heat Transfer," *Heat Transfer*. pp. 1–1015, 2021.
- [15] E. Da Riva, D. Del Col, and A. Cavallini, "Simulation of condensation in a circular minichannel: Application of VOF method and turbulence model," *2010 14th Int. Heat Transf. Conf. IHTC 14*, vol. 2, pp. 205–213, 2010.
- [16] A. A. Abdul-Sahib and A. Muneer, "Experimental steam condensation enhancement on metal foam filled heat exchanger," *J. Mech. Eng. Res. Dev.*, vol. 44, no. 4, pp. 145–167, 2021.